ARTICLES

nature structural biology

Molecular mechanism of Reaper-Grim-Hid-mediated suppression of DIAP1-dependent Dronc ubiquitination

Jijie Chai[1,4], Nieng Yan[1,4], Jun R Huh[2], Jia-Wei Wu[3], Wenyu Li[1], Bruce A Hay[2] & Yigong Shi[1]

The inhibitor of apoptosis protein DIAP1 inhibits Dronc-dependent cell death by ubiquitinating Dronc. The pro-death proteins Reaper, Hid and Grim (RHG) promote apoptosis by antagonizing DIAP1 function. Here we report the structural basis of Dronc recognition by DIAP1 as well as a novel mechanism by which the RHG proteins remove DIAP1-mediated downregulation of Dronc. Biochemical and structural analyses revealed that the second BIR (BIR2) domain of DIAP1 recognizes a 12-residue sequence in Dronc. This recognition is essential for DIAP1 binding to Dronc, and for targeting Dronc for ubiquitination. Notably, the Dronc-binding surface on BIR2 coincides with that required for binding to the N termini of the RHG proteins, which competitively eliminate DIAP1-mediated ubiquitination of Dronc. These observations reveal the molecular mechanisms of how DIAP1 recognizes Dronc, and more importantly, how the RHG proteins remove DIAP1-mediated ubiquitination of Dronc.

Caspases, a family of cysteine proteases that cleave substrates after an aspartate residue, execute cell death by cleaving a broad spectrum of cellular targets[1–3]. The effector caspases are activated by the initiator caspases and are responsible for dismantling the cellular machinery[2]. The activation of the initiator caspases, in turn, is triggered by upstream events[2]. The initiator caspase Dronc has a key role in the onset of programmed cell death (apoptosis) in *Drosophila melanogaster*[4].

The inhibitor of apoptosis (IAP) proteins suppress apoptosis by downregulating caspases[5,6]. IAPs can directly inhibit the catalytic activity of caspases as well as decrease caspase levels; both of these functions depend on physical association. The *Drosophila* inhibitor of apoptosis protein DIAP1 is a potent apoptosis suppressor that is essential for the survival of many cells in the fly[7]. DIAP1 is an E3 ubiquitin ligase and can suppress Dronc-dependent cell death, at least in part, by stimulating Dronc ubiquitination and degradation[8]. During apoptosis, the function of IAPs is compromised by pro-death proteins such as Smac (also known as DIABLO)[9–11] in mammals and Reaper, Hid and Grim (RHG) proteins in *Drosophila*[7]. In mammals, the initiator caspase-9 is activated by Apaf-1 and inhibited by the X-linked IAP (XIAP). The BIR3 domain of XIAP binds to the N-terminal tetrapeptide of the caspase-9 small subunit; this results in the subsequent inhibition of caspase-9 activity[12,13]. During apoptosis, Smac (DIABLO) is released from mitochondria and uses a similar tetrapeptide motif to compete with caspase-9 for binding to XIAP-BIR3, hence removing the inhibition of caspase-9 (ref. 2).

The apoptotic paradigm is highly conserved from flies to mammals. The activation of Dronc, the caspase-9 ortholog in *Drosophila*, is mediated by the large protein Dark (also known as Hac-1 and Dapaf-1), the functional ortholog of the mammalian Apaf-1 (refs. 14–16). Similarly to XIAP in mammals, DIAP1 inhibits Dark- and Dronc-dependent cell death in *Drosophila*[17–19]. However, despite the conservation of apoptotic pathways, the mechanisms by which Dronc and caspase-9 are inhibited seem to be quite different. For example, Dronc lacks the tetrapeptide IAP-binding motif that is present in caspase-9. Thus it is unclear how DIAP1 specifically recognizes Dronc. Consequently, although the pro-apoptotic RHG proteins contain an IAP-binding motif at their N termini and are known to negatively regulate DIAP1 anti-caspase activity and protein levels[20–26], how this is accomplished remains largely unknown. Recent studies on the *Drosophila* IAP-binding protein Jafrac2 suggest that the RHG proteins could displace Dronc from DIAP1 (ref. 27). However, this hypothesis is complicated by the report that the prodomain of Dronc, which contains a CARD motif for homotypic interactions, was responsible for binding to the BIR2 domain of DIAP1 (ref. 28).

In this study, we report that a 12-residue peptide region of Dronc is both necessary and sufficient for binding to the BIR2 domain of DIAP1. Notably, this region (residues 114–125) does not resemble the IAP-binding tetrapeptide motif and is located between the prodomain and the caspase domain of Dronc. Structural analysis of this Dronc fragment bound to the BIR2 domain reveals that the Dronc-binding pocket on BIR2 coincides with that required for binding to the N-terminal sequences of the RHG proteins. Based on this structural finding, we predicted that the RHG proteins competitively eliminate DIAP1-mediated ubiquitination of Dronc by binding to the same conserved surface pocket of DIAP1. We proved this prediction using a combination of genetic and biochemical approaches.

[1]Department of Molecular Biology, Princeton University, Lewis Thomas Laboratory, Washington Road, Princeton, New Jersey 08544, USA. [2]Division of Biology, MC 156-29, California Institute of Technology, Pasadena, California 91125, USA. [3]Department of Biological Sciences and Biotechnology, Tsinghua University, Beijing 100084, China. [4]These authors contributed equally to this work. Correspondence should be addressed to Y. S. (yshi@molbio.princeton.edu).

Published online 28 September 2003; doi:10.1038/nsb989

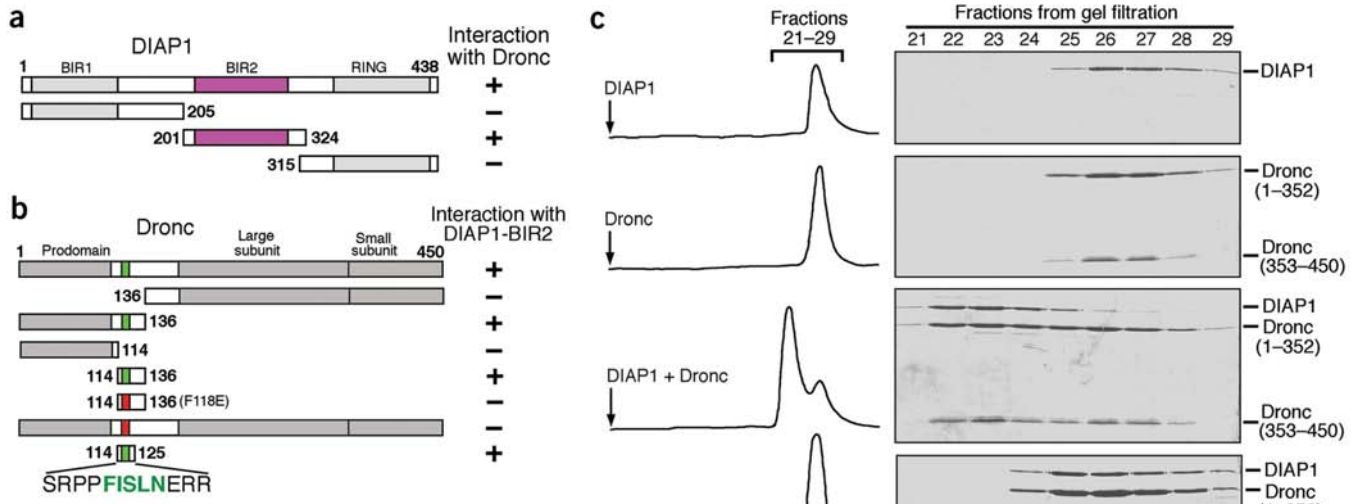

Figure 1 The recognition of Dronc by DIAP1 is restricted to the second BIR domain (BIR2) of DIAP1 and a 12-residue peptide in the linker sequence between the CARD domain and the catalytic subunit of Dronc. (**a**) The DIAP1-BIR2 domain is necessary and sufficient for the interaction with Dronc. The various DIAP1 fragments were purified as fusion proteins with GST. Their interactions with Dronc were examined using both gel filtration and GST-mediated pull-down assays. For details, see Methods. (**b**) A 12-residue peptide of Dronc between the CARD domain and the catalytic subunit was both necessary and sufficient for the interaction with DIAP1. (**c**) A representative interaction between the full-length DIAP1 and Dronc is shown. A single missense mutation (F118E) in Dronc was sufficient to disrupt the DIAP1-Dronc interactions. The chromatograms of gel filtration and the relevant fractions are shown. In the bottom panel, although DIAP1 and Dronc (F118E) appeared to co-elute, there was no detectable interaction, because the elution volume for each individual protein in the 'complex' is essentially the same as for the isolated protein alone.

RESULTS

Recognition of Dronc by DIAP1

To understand the molecular mechanisms of Dronc regulation by DIAP1 and the RHG proteins, we examined pairwise interactions between fragments of Dronc, DIAP1 and the RHG proteins. Results derived from GST pull-down assays and gel filtration analyses (data not shown) (**Fig. 1a**) demonstrated that the second BIR (BIR2) domain of DIAP1 (residues 201–324) was both necessary and sufficient for binding to the pro-Dronc zymogen (C318A) or the active Dronc protein cleaved after Glu352. In contrast, neither the BIR1 domain (residues 1–205) nor the RING domain (residues 315–438) had any detectable interaction with Dronc.

Next, we examined the minimal sequence requirement of Dronc for stable interactions with DIAP1. Notably, neither the protease domain (residues 136–450) nor the N-terminal CARD (prodomain) of Dronc (residues 1–114) bound to the BIR2 domain (**Fig. 1b**). Rather, a short 12-residue fragment (residues 114–125) between the CARD and the protease domain of Dronc formed a stable complex with DIAP1-BIR2. This result is in contrast to a previous report in which the CARD domain of Dronc was reported to interact with DIAP1; however, the amino acid boundaries of the CARD domain were not given in that study[28].

Quantification of gel filtration experiments revealed the binding affinity to be ~0.8 μM between DIAP1-BIR2 (residues 201–324) and Dronc (residues 1–136) (data not shown). A similar binding affinity (~0.9 μM) was obtained for the full-length DIAP1 and Dronc (data not shown). These binding affinities were further confirmed by preliminary BiaCore measurements (data not shown) and are comparable to the XIAP-caspase-9 and XIAP-Smac interactions[12,29]. To demonstrate the specificity of this interaction, we carried out extensive mutagenesis on this peptide region, in which every amino acid between residues 114 and 125 was mutated to either alanine or glutamate. Based on both GST pull-down assays and gel filtration analyses (data not shown), any mutation of Phe118, Ile119, Leu121 or Asn122 weakened or abolished the Dronc-DIAP1 interaction whereas mutations outside residues 118–122 had no detectable effect on the interaction. These results indicate that amino acids 118–122 of Dronc directly contribute to DIAP1 binding. Within this peptide region, a single missense mutation in Dronc, F118E, resulted in a loss of interaction with DIAP1 (**Fig. 1b,c**), suggesting an indispensable role for this residue in binding to DIAP1.

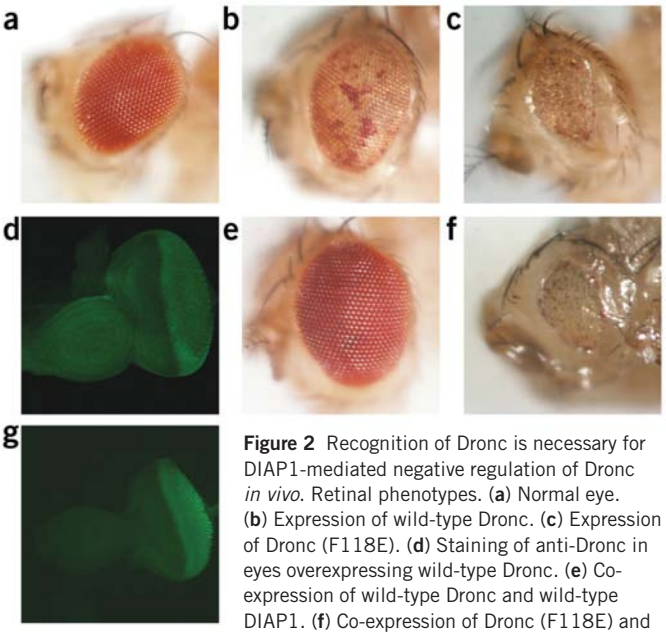

Figure 2 Recognition of Dronc is necessary for DIAP1-mediated negative regulation of Dronc *in vivo*. Retinal phenotypes. (**a**) Normal eye. (**b**) Expression of wild-type Dronc. (**c**) Expression of Dronc (F118E). (**d**) Staining of anti-Dronc in eyes overexpressing wild-type Dronc. (**e**) Co-expression of wild-type Dronc and wild-type DIAP1. (**f**) Co-expression of Dronc (F118E) and wild-type DIAP1. (**g**) Staining of anti-Dronc in eyes overexpressing Dronc (F118E).

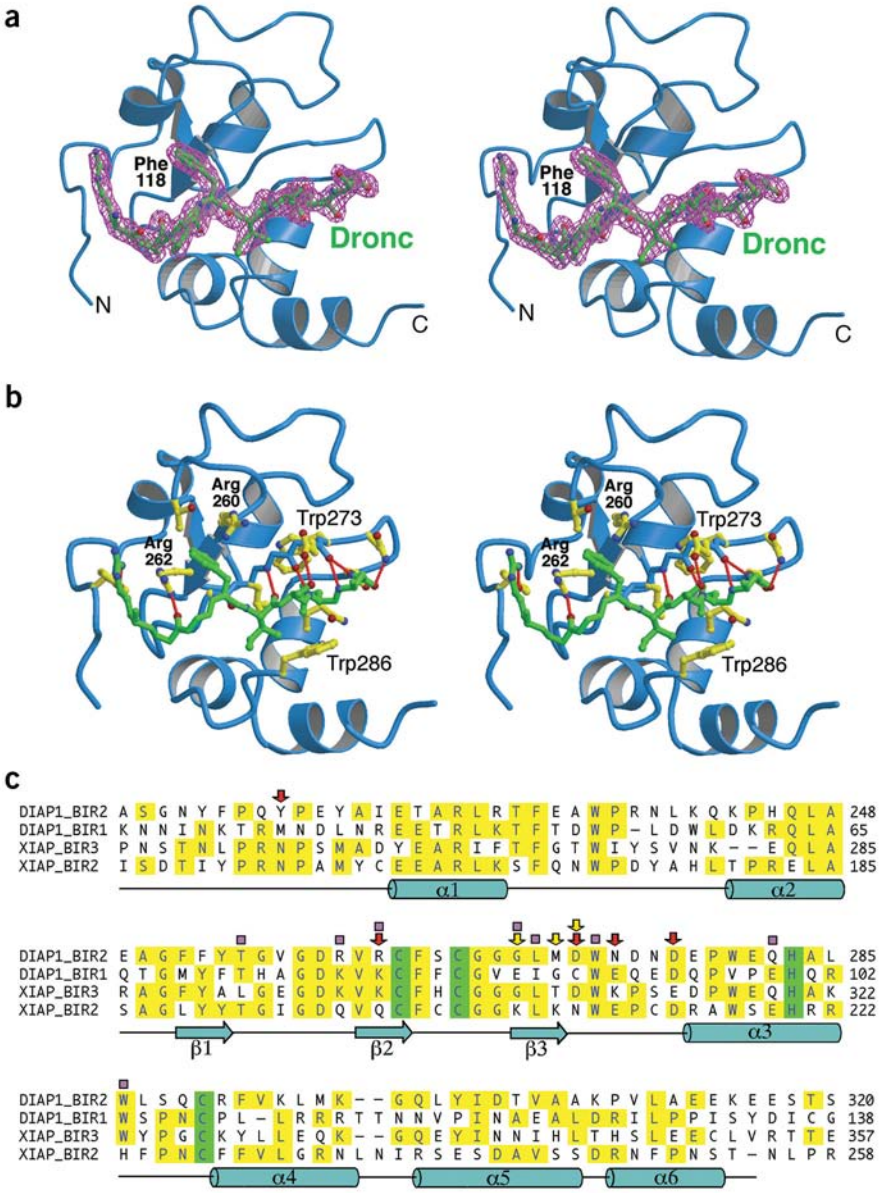

Figure 3 Structural mechanism of Dronc recognition by DIAP1. (**a**) Structure of DIAP1-BIR2 domain in complex with a ten-residue Dronc peptide in stereo view. The BIR2 domain and the Dronc peptide are blue and green, respectively. The omit electron density map, shown at 1.5 σ and colored pink, was calculated using the CNS[37]. (**b**) Stereo representation of interactions between the Dronc peptide and the BIR2 domain of DIAP1. The residues from Dronc and DIAP1 are green and yellow, respectively. Hydrogen bonds are red dashed lines. (**c**) Sequence alignment of the BIR domains from DIAP1 and XIAP. The zinc-chelating residues are green whereas the conserved amino acids are yellow. Red and yellow arrows identify those residues that make intermolecular hydrogen bonds using their side chain and main chain atoms, respectively. The secondary structural elements for the DIAP1-BIR2 domain are indicated below the sequence alignment. This figure and **Figure 4a** were prepared using MOLSCRIPT[40].

Significance of Dronc-DIAP1 interaction

To examine the biological significance of the Dronc-DIAP1 interaction, we generated transgenic flies overexpressing either the wild-type Dronc or the mutant Dronc (F118E) under the eye-specific glass promoter. In contrast to the wild-type eyes (**Fig. 2a**), expression of both versions of Dronc led to retinal degeneration, though flies with the mutant Dronc (F118E) consistently showed a stronger eye ablation phenotype than those flies expressing wild-type Dronc (**Fig. 2b,c** and J.R.H. and B.A.H., unpublished observations). This is likely due to the fact that the mutant Dronc was no longer subjected to negative regulation by the endogenous DIAP1 protein. As anticipated, the wild-type Dronc protein was expressed at high levels in the eyes (**Fig. 2d**). The retinal cell death phenotype of flies expressing the wild-type Dronc was suppressed by co-expression of the full-length DIAP1 (**Fig. 2e**). In sharp contrast, the phenotype associated with expression of Dronc (F118E), which no longer interacts with DIAP1, could not be rescued by DIAP1 (**Fig. 2f**).

The inability of the wild-type DIAP1 to suppress the mutant Dronc (F118E) phenotype was not due to a higher expression level, because both wild type and the mutant Dronc were present at similar levels in the fly eyes, as determined by the staining intensity of green fluorescence protein–labeled anti-Dronc antibody (**Fig. 2d,g**). In addition, both Dronc proteins had an identical enzymatic activity in an *in vitro* assay using TQTE-AFC as the substrate (data not shown). The only difference between these two Dronc proteins is that the mutant (F118E) can no longer be recognized by its negative regulator DIAP1. Consequently, the mutant Dronc remained stable in the presence of DIAP1 as determined by western blots (data not shown). Thus, these observations demonstrate that interactions between DIAP1-BIR2 and the Dronc peptide are essential for the negative regulation of Dronc by DIAP1.

Structure of a DIAP1–Dronc complex

To reveal the molecular basis of Dronc recognition by DIAP1, we generated and crystallized the binary complex between the DIAP1-BIR2 domain (residues 201–324) and a ten-residue Dronc peptide (residues 114–123). The structure was determined by molecular replacement and refined to a resolution of 2.1 Å with a crystallographic *R*-factor of 19.9% (**Table 1** and **Fig. 3a**).

The Dronc peptide adopts an extended conformation and binds to a hydrophobic surface groove on the BIR2 domain, making multiple specific interactions with DIAP1 residues. There are numerous intermolecular van der Waals contacts and 12 hydrogen bonds between the BIR2 domain and the bound Dronc peptide (**Fig. 3b,c**). Although the Dronc peptide contains ten amino acids, only five contiguous residues (Phe118–Asn122) make extensive contacts to the BIR2 residues. Among these five residues, three hydrophobic amino acids (Phe118, Ile119 and Leu121) seem to anchor the binding to DIAP1 through networks of van der Waals interactions. The other two residues, Ser120 and Asn122, facilitate binding through specific hydrogen bonds (**Fig. 3b,c**).

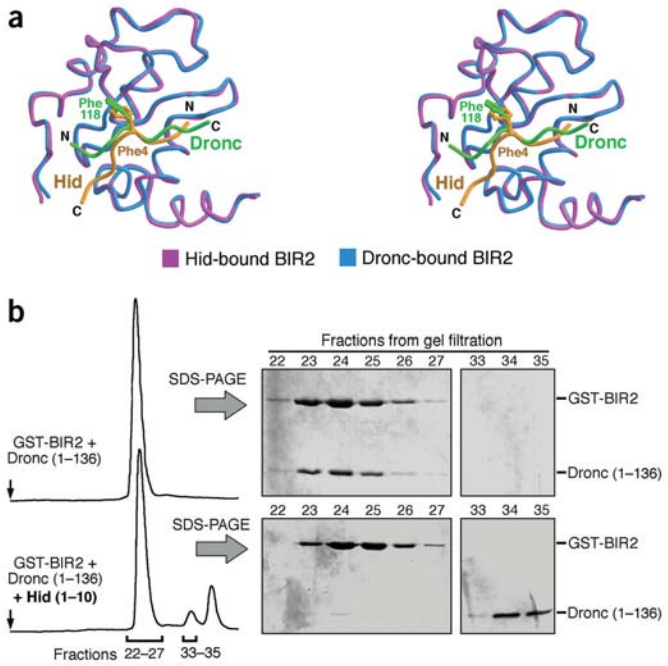

Figure 4 Dronc and Hid compete with each other for binding to the same surface groove on the BIR2 domain of DIAP1. (**a**) Stereo superposition of the structures of DIAP1-BIR2 bound to Dronc and to Hid peptide. The Dronc and Hid peptides are green and orange, respectively. Note the difference in the orientation of the two peptides. Phe118 of Dronc and Phe4 of Hid occupy the same general pocket on the surface of DIAP1. (**b**) A ten-residue peptide derived from the N terminus of Hid disrupts the interaction between Dronc and DIAP1. GST-BIR2-Dronc (1–136) complex (1.2 mg) was used for each gel filtration run. Hid peptide (60 μg) was used to disrupt the BIR2–Dronc complex. The chromatograms for gel filtration are on the left and the relevant fractions from gel filtration were visualized by SDS-PAGE and stained with Coomassie blue.

These structural observations are fully supported by our mutagenesis studies. Phe118 in Dronc, whose mutation to glutamate resulted in complete disruption of interaction with DIAP1, resides at the center of the interface. The aromatic side chain of Phe118 is nestled in the hydrophobic pocket formed by Thr255, Gly269 and the aliphatic side chains of Arg260 and Arg262 (**Fig. 3b**).

Mutual exclusion of Dronc and the RHG proteins

The conserved peptide-binding pocket on the surface of BIR domains has been defined for a number of mammalian IAPs and for the *Drosophila* DIAP1 (refs. 30,31). The general principle was thought to be that the N-terminal residue of the bound peptide must be alanine with a free N terminus[29,32]. In addition, all known IAP-binding motifs share a conserved tetrapeptide sequence[31]. Because Dronc does not contain such a tetrapeptide motif, it was not expected to occupy the conserved surface groove of DIAP1-BIR2. However, to our complete surprise, the Dronc peptide binds to the same surface groove as the N-terminal sequences of Reaper, Hid and Grim. The side chain of Phe118 from Dronc occupies the same position as that of Phe4 from the Hid protein[30] (**Fig. 4a**) or Tyr4 from Grim[30].

The conformation of the conserved surface groove on DIAP1-BIR2 remains unchanged before and after binding to the RHG proteins[30]. How can the conserved and rigid surface groove on DIAP1 accommodate the Dronc peptide, which is different from the canonical IAP-binding tetrapeptide motif? Comparative analysis revealed an answer to this question. Compared with Hid or Grim, the Dronc peptide binds to DIAP1-BIR2 in a reverse orientation, with the N terminus of the Dronc peptide close to the C-terminal portion of the Hid peptide (**Fig. 4a**). Except for the phenylalanine residue, the Dronc peptide has no resemblance to the N-terminal sequences of Reaper, Hid or Grim. As will be seen below, the accommodation of two different kinds of peptide by the BIR2 domain is central to the anti-apoptotic function of DIAP1 and to the pro-apoptotic function of Reaper, Hid and Grim.

Based on this unanticipated structural finding, we predicted that the pro-apoptotic proteins Reaper, Hid, Grim and Sickle should be able to disrupt the DIAP1-Dronc interaction by binding to the same surface groove of DIAP1, hence removing DIAP1-mediated Dronc ubiquitination. This prediction is supported by the observation that the RHG proteins interact with DIAP1-BIR2 with 0.041–0.24 μM binding affinities[30], higher than that between DIAP1 and Dronc (~0.8 μM).

To further corroborate the structural prediction, we examined whether the N-terminal peptide derived from Hid could disrupt the interaction between DIAP1 and Dronc using gel filtration. In the absence of Hid, GST-DIAP1-BIR2 formed a stable complex with the Dronc fragment 1–136 (**Fig. 4b**). Incubation with 60 μg of the Hid peptide (residues 1–10, approximately two-fold in excess) resulted in a complete disruption of the DIAP1–Dronc complex (**Fig. 4b**). Similar results were obtained for the other three pro-death proteins Reaper, Grim and Sickle (data not shown).

Removal of DIAP1-mediated ubiquitination

To demonstrate that Reaper, Hid, Grim, Sickle and Jafrac2-like proteins indeed remove DIAP1-mediated Dronc ubiquitination by outcompeting Dronc peptide for binding to DIAP1, we reconstituted an *in vitro* ubiquitination assay using highly purified recombinant ubiquitin activating enzyme (E1), ubiquitin conjugating enzyme (E2), DIAP1 (E3), ubiquitin and the Dronc substrate (C318A) (**Fig. 5a**). To eliminate undesirable protease activity (from Dronc) in this assay, the

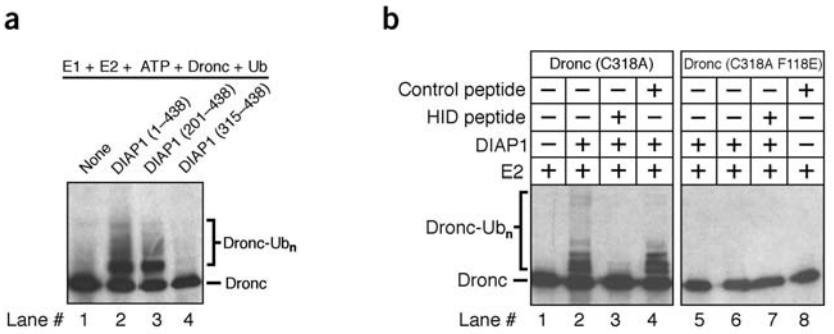

Figure 5 Molecular mechanism of the removal of DIAP1-mediated Dronc ubiquitination by the pro-apoptosis protein Hid. (**a**) The BIR2 domain is required for the ubiquitination of Dronc *in vitro*. Various DIAP1 fragments were examined for their E3 ubiquitin ligase activity in the ubiquitination reaction of Dronc (C318A). The gel was blotted using an anti-Dronc raised against its CARD domain. E1, E2, Dronc (C318A) and DIAP1 were individually purified to homogeneity as described in Methods. (**b**) A ten-residue peptide derived from the N terminus of Hid specifically removes DIAP1-mediated ubiquitination of Dronc. The control peptide has the sequence N-DYPDQNRRRIGAEK-C.

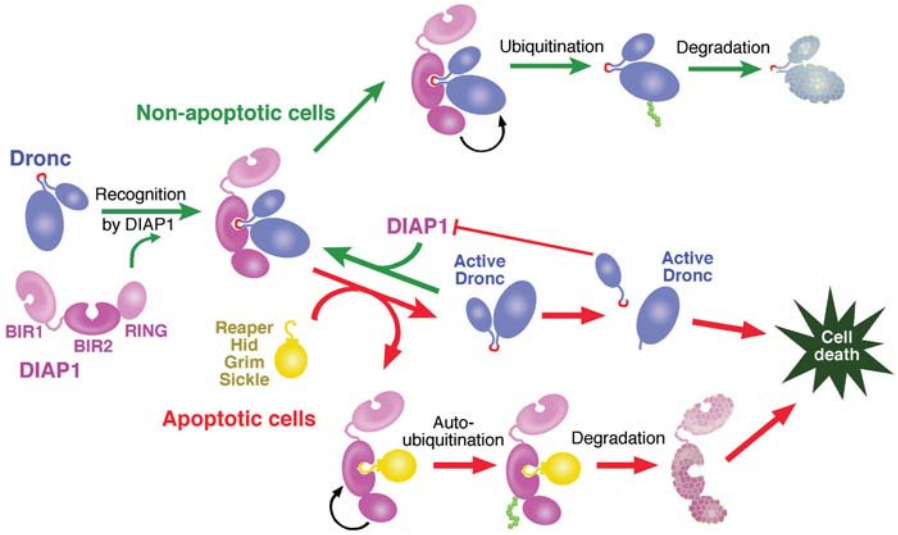

Figure 6 A schematic representation of the regulation of Dronc by DIAP1 and the RHG proteins. In non-apoptotic cells, DIAP1 interacts with Dronc and keeps its level low through ubiquitination. In apoptotic cells, the RHG proteins compete with Dronc for binding to the same surface groove on the BIR2 domain of DIAP1, hence removing DIAP1-mediated Dronc ubiquitination. Dronc activates downstream caspases that feed back to cleave off the DIAP1-binding peptide from the mature protease domain of Dronc. This form of Dronc is no longer regulated by DIAP1. In addition, the cleaved N-terminal fragment of Dronc serves as an inert decoy to bind to DIAP1, making it unable to recognize or ubiquitinate Dronc.

catalytic residue Cys318 was mutated to alanine in the substrate Dronc. In the absence of DIAP1, the reaction resulted in only a background level of ubiquitination (**Fig. 5a**, lane 1). In contrast, incubation with DIAP1 led to efficient ubiquitination of Dronc (lane 2). As anticipated, this reaction required both the BIR2 domain, for Dronc recognition, and the RING domain, for ubiquitin transfer from E2 to the substrate Dronc (lanes 2 and 3). Removal of the BIR1 domain had no detectable effect on the ubiquitination of Dronc (lane 3). In agreement with our biochemical observations, removal of the BIR2 domain resulted in complete abrogation of Dronc ubiquitination (lane 4). The same conclusion was obtained when the wild-type Dronc protein was used as the substrate (data not shown).

Then we examined the effect of the pro-apoptosis proteins Reaper, Hid, Grim and Sickle on the DIAP1-mediated ubiquitination of Dronc (C318A) (**Fig. 5b**). As predicted by the structural finding, incubation with the Hid peptide (lane 3, 2 μg) but not a control peptide (lane 4, 2 μg) efficiently removed the DIAP1-dependent ubiquitination of Dronc. The same conclusion was obtained using the N-terminal peptides derived from Reaper, Grim and Sickle (data not shown). Finally, we examined the ubiquitination of the mutant Dronc (C318A F118E), which no longer interacts with DIAP1. Compared to Dronc (C318A) (lane 2), DIAP1 failed to substantially augment the ubiquitination of this mutant Dronc (lane 6). More importantly, incubation with the Hid peptide had no effect on the ubiquitination of this mutant Dronc (lane 8). This is also apparent by comparing the result to that using a control peptide (lane 7). These results also provide a mechanistic explanation to the observed eye phenotypes (**Fig. 2**).

DISCUSSION

Our results indicate that the pro-apoptotic proteins Reaper, Hid, Grim and Sickle use distinct strategies to promote Dronc-dependent cell death. In addition to downregulating DIAP1 levels relative to those of caspase targets[20–24], they prevent DIAP1 from stimulating the ubiquitination of Dronc (**Fig. 6**). This activity is strictly dependent on the mutual exclusion of Dronc and the RHG proteins for binding to DIAP1, which in turn ensures that Dronc does not get 'accidentally' degraded owing to the negative regulation of DIAP1 levels. The essential DIAP1-binding sequence in Dronc (residues 118–122) precedes two caspase cleavage sites, 132-DIVD-135 for DrICE and DCP-1 and 140-EASE-143 for Dronc. Thus caspase-mediated cleavage of Dronc during apoptosis will release the N-terminal IAP-binding fragment from the protease domain of Dronc, allowing the active Dronc to activate downstream caspases in an IAP-independent manner (**Fig. 6**). In addition, the cleaved N-terminal fragment of Dronc could serve as an inert decoy to bind to DIAP1, making it unable to recognize or ubiquitinate Dronc (**Fig. 6**). This arrangement could constitute a positive feedback regulation on Dronc activity during apoptosis (**Fig. 6**). This hypothesis would represent a novel mechanism for the positive feedback amplification of caspase activation. A similar mechanism has been proposed for the activation of the mammalian caspase-9 involving cleavage at Asp330 (ref. 13); however, recent data showed that after Asp330 cleavage, the resulting caspase-9 was still efficiently bound and inhibited by XIAP[12,33].

In this study, we uncovered the molecular mechanism for the specific recognition of Dronc by the *Drosophila* DIAP1. This mechanism is supported by a combination of biochemical, developmental and structural data. The structural finding revealed a novel mechanism by which the pro-apoptotic RHG proteins antagonize DIAP1-mediated suppression of Dronc. The rigid surface pocket on the BIR2 domain of DIAP1 serves at least two purposes, to accommodate the Dronc peptide so as to inhibit apoptosis under non-apoptotic conditions, and to accommodate the N-terminal peptides from the pro-death proteins Reaper, Hid, Grim, Sickle and Jafrac2 during apoptosis to facilitate cell death (**Fig. 6**).

Although the general paradigm of apoptosis is conserved from mammals to flies, the mechanism of regulation seems to be highly divergent. For example, the binding of caspase-9 by XIAP results in its inhibition. Yet DIAP1-mediated binding of Dronc does not affect its catalytic activity (N.Y. and Y.S., unpublished data). Rather, the only DIAP1-dependent negative regulation of Dronc known so far is its ubiquitination and subsequent degradation. The RHG proteins use their N termini to counter DIAP1-mediated negative regulation of Dronc. Compared with the mammalian paradigm, the *Drosophila* cases are particularly notable as the internal peptide of Dronc does not resemble the canonical IAP-binding motif[30,31] yet binds to the same surface pocket of DIAP1 (**Fig. 4**). This notable physical interaction is essential to the function of DIAP1 as well as those of the pro-apoptosis proteins Reaper, Hid, Grim and Sickle. Binding of DIAP1 by a peptide in Dronc that is unrelated to the documented IAP-binding motif indicates that other classes of IAP-binding motifs have a physiologically critical role in mediating or antagonizing IAP function and this paradigm may apply to other species.

Table 1 Data collection and refinement

Data collection	
Beamline	CHESS-A1
Space group	$P6_5$
Resolution (Å)	99.0–2.1
Total observations	582,663
Unique observations	94,061
Data coverage (%)[a]	94.2 (82)
R_{sym}[a,b]	0.057 (0.173)
Refinement	
Resolution range (Å)	20.0–2.1
Number of reflections ($\|F\| > 0$)	93,347
Data coverage (%)[a]	93.0 (80)
R_{work}[c]	0.199
R_{free}[c]	0.246
Number of atoms	9,167
Number of waters	557
R.m.s. deviations[d]	
Bond length (Å)	0.009
Bond angle (°)	1.531

[a]Values in parentheses are for the highest-resolution shell. [b]$R_{sym} = \Sigma_h \Sigma_i | I_{h,i} - I_h | / \Sigma_h \Sigma_i I_{h,i}$, where I_h is the mean intensity of the i observations of symmetry-related reflections of h. [c]$R = \Sigma | F_o - F_c | / \Sigma F_o$, where $F_o = F_P$, and F_c is the calculated protein structure factor from the atomic model (R_{free} was calculated with 5% of the reflections). [d]R.m.s. deviations of bond lengths and angles are the deviations from ideal values, and the r.m.s. deviation of B-factors is calculated between bonded atoms.

METHODS

Protein and peptide preparation. All constructs were generated using a standard PCR-based cloning strategy, and the identities of individual clones were verified through double-stranded plasmid sequencing. For interaction assays, all of the proteins were overexpressed in *Escherichia coli* strain BL21(DE3) either as GST-fusion proteins using pGEX-2T (Pharmacia), or as C-terminal His_6-tagged proteins using pET21b (Novagen). Proteins were purified to homogeneity as described[30]. The ten-residue Reaper, Grim, Hid, Sickle and Dronc peptides were chemically synthesized, purified by reverse phase HPLC, lyophilized and resuspended in buffer. For crystallization, the homogeneous DIAP1-BIR2 domain was mixed with equimolar amount of Dronc peptide and diluted to a final concentration of 10 mg ml^{-1}.

Crystallization and data collection. Crystals of DIAP1-BIR2 (residues 201–324) in complex with the Dronc peptide were obtained by hanging-drop vapor diffusion by mixing the complex (10 mg ml^{-1}) with an equal volume of reservoir solution containing 100 mM sodium citrate, pH 5.8, 15% (w/v) PEG4000 (w/v) and 120 mM ammonium sulfate. Crystals, with a typical dimension of $0.05 \times 0.05 \times 0.08$ mm^3, are in the space group $P6_5$ and contain ten complexes in each asymmetric unit. The unit cell dimensions are $a = b =$ 128.9 Å, and $c = 183.7$ Å. Macroseeding yielded crystals with a maximum size of $0.2 \times 0.2 \times 0.4$ mm^3 over a period of 6–7 d. Crystals were equilibrated in a cryoprotectant buffer containing well buffer plus 20% (v/v) glycerol, and were flash frozen in a –170 °C nitrogen stream. The native data were collected at the CHESS beamline A1 (Ithaca, New York, USA). Data were processed using DENZO and SCALEPACK[34].

Structure determination. The structure was determined by molecular replacement, using AMoRe[35]. The atomic model was built using O[36] and refined using CNS[37]. The electron density for the bound peptide fragments became unambiguous after preliminary refinement. The final refined atomic model contains residues 216–309 of DIAP1 and residues 115–122 of Dronc at a resolution of 2.1 Å. The N-terminal 15 residues and the C-terminal 15 residues in DIAP1-BIR2 have no electron density in the maps, and we presume that these regions are disordered in the crystals.

Gel filtration assay. Individual recombinant proteins were purified to more than 95% homogeneity and incubated in assay buffer (25 mM Tris, pH 8.0, 150 mM NaCl and 2 mM DTT). The protein mixture (0.5 ml) was subjected to gel filtration analysis (Superdex 200, Amersham-Pharmacia) for each run. Samples taken from relevant fractions were visualized by SDS-PAGE with Coomassie blue staining. For an estimate of the binding affinity between Dronc (residues 1–136) and DIAP1 (residues 201–324), 200 µl of Dronc (4 µM) and 200 µl of DIAP1 (4 µM) were incubated at 4 °C for 30 min before the mixture was subjected to gel filtration analysis. The fractions of free and bound proteins, visualized by SDS-PAGE and quantified by densitometry, were used to estimate the dissociation constant.

GST-mediated pull-down assay. Approximately 0.4 mg of a recombinant DIAP1 (or Dronc) variant was bound to 200 µl of glutathione resin as a GST-fusion protein. The resin was washed with 400 µl buffer four times to remove excess unbound protein or other contaminants. Then 600 µg of the Dronc (or DIAP1) protein was allowed to flow through the resin. After extensive washing with an assay buffer containing 25 mM Tris, pH 8.0, 150 mM NaCl, and 2 mM DTT, GST-DIAP1 was eluted with 5 mM reduced glutathione and all fractions were visualized by SDS-PAGE with Coomassie blue staining.

***In vitro* ubiquitination assay.** Reactions were carried out at 37 °C. Approximately 20–100 ng of E1 (ubiquitin activating enzyme), 0.5–2 µg of E2 (UbcH5, ubiquitin conjugating enzyme), 2 µg of ubiquitin (SIGMA) and 1–5 µg of recombinant DIAP1 or its fragments and 5 µg substrate Dronc proteins were incubated in assay buffer (25 mM Tris, pH 7.5, 5 mM $MgCl_2$, 2 mM ATP, 0.5 mM DTT, 0.05% (v/v) NP-40) for 30 min. Then the products were applied to SDS-PAGE, transferred to nitrocellulose membrane and visualized by western blot using a polyclonal antibody raised against a Dronc peptide (residues 325–351). To eliminate background Dronc ubiquitination that is independent of DIAP1-Dronc interactions (in **Fig. 5b**), we titrated the amount of E3 (DIAP1) in these reactions. DIAP1 (≤20 ng) was found to give rise to an undetectable level of background ubiquitination.

***Drosophila* genetics and immunocytochemistry.** GMR-Dronc-WT and GMR-DIAP1 have been previously described[38,39]. GMR-Dronc-F118E flies were generated by introducing Dronc-F118E into the GMR P-element vector and then introducing this construct into the *Drosophila* germline using standard techniques. Multiple lines were generated. These lines consistently had retinal degeneration phenotypes stronger than those of GMR-Dronc-WT flies. Anti-Dronc staining was carried out on third instar eye discs from flies of various genotypes essentially as described[20]. Rabbit anti-Dronc was used at a dilution of 1:5,000.

Coordinates. The atomic coordinates have been deposited in the Protein Data Bank (accession code 1Q4Q).

ACKNOWLEDGMENTS

We thank L. Walsh and others at CHESS for help with beam time and data collection. This research was supported by US National Institutes of Health grants.

COMPETING INTERESTS STATEMENT

The authors declare that they have no competing financial interests.

Received 26 June; accepted 13 August 2003
Published online at http://www.nature.com/naturestructuralbiology/

1. Thornberry, N.A. & Lazebnik, Y. Caspases: enemies within. *Science* **281**, 1312–1316 (1998).
2. Shi, Y. Mechanisms of caspase inhibition and activation during apoptosis. *Mol. Cell* **9**, 459–470 (2002).
3. Earnshaw, W.C., Martins, L.M. & Kaufmann, S.H. Mammalian caspases: structure, activation, substrates, and functions during apoptosis. *Annu. Rev. Biochem.* **68**, 383–424 (1999).
4. Quinn, L.M. *et al.* An essential role for the caspase Dronc in developmentally programmed cell death in *Drosophila*. *J. Biol. Chem.* **275**, 40416–40424 (2000).
5. Deveraux, Q.L. & Reed, J.C. IAP family proteins—suppressors of apoptosis. *Genes Dev.* **13**, 239–252 (1999).
6. Salvesen, G.S. & Duckett, C.S. IAP proteins: blocking the road to death's door. *Nat. Rev. Mol. Cell Biol.* **3**, 401–410 (2002).
7. Hay, B.A. Understanding IAP function and regulation: a view from *Drosophila*. *Cell Death Differ.* **7**, 1045–1056 (2000).
8. Wilson, R. *et al.* The DIAP1 RING finger mediates ubiquitination of Dronc and is

indispensable for regulating apoptosis. *Nat. Cell Biol.* **4**, 445–450 (2002).
9. Du, C., Fang, M., Li, Y. & Wang, X. Smac, a mitochondrial protein that promotes cytochrome c-dependent caspase activation during apoptosis. *Cell* **102**, 33–42 (2000).
10. Verhagen, A.M. *et al.* Identification of DIABLO, a mammalian protein that promotes apoptosis by binding to and antagonizing IAP proteins. *Cell* **102**, 43–53 (2000).
11. Chai, J. *et al.* Structural and biochemical basis of apoptotic activation by Smac/DIABLO. *Nature* **406**, 855–862 (2000).
12. Shiozaki, E.N. *et al.* Mechanism of XIAP-mediated inhibition of caspase-9. *Mol. Cell* **11**, 519–527 (2003).
13. Srinivasula, S.M. *et al.* A conserved XIAP-interaction motif in caspase-9 and Smac/DIABLO mediates opposing effects on caspase activity and apoptosis. *Nature* **409**, 112–116 (2001).
14. Kanuka, H. *et al.* Control of the cell death pathway by Dapaf-1, a *Drosophila* Apaf-1/CED-4-related caspase activator. *Mol. Cell* **4**, 757–769 (1999).
15. Zhou, L., Song, Z., Tittel, J. & Steller, H. HAC-1, a *Drosophila* homolog of Apaf-1 and CED-4 functions in developmental and radiation-induced apoptosis. *Mol. Cell* **4**, 745–755 (1999).
16. Rodriguez, A. *et al.* Dark is a *Drosophila* homologue of Apaf-1/CED-4 and functions in an evolutionarily conserved death pathway. *Nat. Cell Biol.* **1**, 272–279 (1999).
17. Rodriguez, A., Chen, P., Oliver, H. & Abrams, J.M. Unrestrained caspase-dependent cell death caused by loss of Diap1 function requires the *Drosophila* Apaf-1 homolog, Dark. *EMBO J.* **21**, 2189–2197 (2002).
18. Zimmermann, K.C., Ricci, J.E., Droin, N.M. & Green, D.R. The role of ARK in stress-induced apoptosis in *Drosophila* cells. *J. Cell Biol.* **156**, 1077–1087 (2002).
19. Muro, I., Hay, B.A. & Clem, R.J. The *Drosophila* DIAP1 protein is required to prevent accumulation of a continuously generated, processed form of the apical caspase DRONC. *J. Biol. Chem.* **277**, 49644–49650 (2002).
20. Yoo, S.J. *et al.* Hid, Rpr and Grim negatively regulate DIAP1 levels through distinct mechanisms. *Nat. Cell Biol.* **4**, 416–424 (2002).
21. Hays, R., Wickline, L. & Cagan, R. Morgue mediates apoptosis in the *Drosophila melanogaster* retina by promoting degradation of DIAP1. *Nat. Cell Biol.* **4**, 425–431 (2002).
22. Ryoo, H.D., Bergmann, A., Gonen, H., Ciechanover, A. & Steller, H. Regulation of *Drosophila* IAP1 degradation and apoptosis by reaper and ubcD1. *Nat. Cell Biol.* **4**, 432–438 (2002).
23. Holley, C.L., Olson, M.R., Colon-Ramos, D.A. & Kornbluth, S. Reaper eliminates IAP proteins through stimulated IAP degradation and generalized translational inhibition. *Nat. Cell Biol.* **4**, 439–444 (2002).
24. Wing, J.P. *et al. Drosophila* Morgue is an F box/ubiquitin conjugase domain protein important for grim-reaper mediated apoptosis. *Nat. Cell Biol.* **4**, 451–456 (2002).
25. Goyal, L., McCall, K., Agapite, J., Hartwieg, E. & Steller, H. Induction of apoptosis by *Drosophila* reaper, hid and grim through inhibition of IAP function. *EMBO J.* **19**, 589–597 (2000).
26. Wang, S., Hawkins, C., Yoo, S., Muller, H.-A. & Hay, B. The *Drosophila* caspase inhibitor DIAP1 is essential for cell survival and is negatively regulated by HID. *Cell* **98**, 453–463 (1999).
27. Tenev, T., Zachariou, A., Wilson, R., Paul, A. & Meier, P. Jafrac2 is an IAP antagonist that promotes cell death by liberating Dronc from DIAP1. *EMBO J.* **21**, 5118–5129 (2002).
28. Meier, P., Silke, J., Leevers, S.J. & Evan, G.I. The *Drosophila* caspase DRONC is regulated by DIAP1. *EMBO J.* **19**, 598–611 (2000).
29. Liu, Z. *et al.* Structural basis for binding of Smac/DIABLO to the XIAP BIR3 domain. *Nature* **408**, 1004–1008 (2000).
30. Wu, J.-W., Cocina, A.E., Chai, J., Hay, B.A. & Shi, Y. Structural analysis of a functional DIAP1 fragment bound to Grim and Hid peptides. *Mol. Cell* **8**, 95–104 (2001).
31. Shi, Y. A conserved tetrapeptide motif: potentiating apoptosis through IAP-binding. *Cell Death Differ.* **9**, 93–95 (2002).
32. Wu, G. *et al.* Structural basis of IAP recognition by Smac/DIABLO. *Nature* **408**, 1008–1012 (2000).
33. Zou, H. *et al.* Regulation of the Apaf-1/caspase-9 apoptosome by caspase-3 and XIAP. *J. Biol. Chem.* **278**, 8091–8098 (2003).
34. Otwinowski, Z. & Minor, W. Processing of X-ray diffraction data collected in oscillation mode. *Methods Enzymol.* **276**, 307–326 (1997).
35. Navaza, J. AMoRe and automated package for molecular replacement. *Acta Crystallogr. A* **50**, 157–163 (1994).
36. Jones, T.A., Zou, J.-Y., Cowan, S.W. & Kjeldgaard, M. Improved methods for building protein models in electron density maps and the location of errors in these models. *Acta Crystallogr. A* **47**, 110–119 (1991).
37. Terwilliger, T.C. & Berendzen, J. Correlated phasing of multiple isomorphous replacement data. *Acta Crystallogr. D* **52**, 749–757 (1996).
38. Hawkins, C.J. *et al.* The *Drosophila* caspase DRONC cleaves following glutamate or aspartate and is regulated by DIAP1, HID, and GRIM. *J. Biol. Chem.* **275**, 27084–27093 (2000).
39. Hay, B.A., Wassarman, D.A. & Rubin, G.M. *Drosophila* homologs of baculoviral inhibitor of apoptosis proteins function to block cell death. *Cell* **83**, 1253–1262 (1995).
40. Kraulis, P.J. MOLSCRIPT: a program to produce both detailed and schematic plots of protein structures. *J. Appl. Crystallogr.* **24**, 946–950 (1991).